Optical Geometric Properties of Skin Epidermis Surface: Statistical and Fractal Approach

Angelsky O.V., [1]Ushenko A.G. and Ushenko Yu.A.

Correlation Optics Department, Chernivtsi National University, 2 Kotsyubinsky St., 58012 Chernivtsi, Ukraine E-mail:ushenko-bio@itf.cv.ukrtel.net

Received:21.12.2005

Abstract

Interrelation between the polarization state of local zones of the object field and the inclination angles of skin epidermis plates has been found within a single-scattering approximation. The technique for the polarization reconstruction of coordinate distribution of the inclination angles of surface micro-irregularities referred to the skin epidermis has been suggested. The first-to-fourth orders statistics for the optical geometric properties of rough surface of physiologically normal and pathologically changed skins has been analyzed. It has been shown that the microrelief of the healthy skin surface has a fractal angular structure. Pathological changes cause random distribution of the inclination angles of the skin surface micro-irregularities.

Keywords: biological tissue, statistical moments, power spectrum.

PACS: 42.62.-b, 42.62.Be, 42.25.Lc, 42.25.Ja, 81.70.Tx

1. Introduction

Investigation of optical geometric structure of human skin is one of important directions in biological tissue optics [1]. In their spectrophotometric aspects, the problems of light scattering by such objects have been analyzed in detail with the aid of Monte-Carlo technique. This statistical modelling enables one to determine the intensity distributions for the Gaussian-profile beams, with taking into account both the experimental geometry and the optical properties of objects under test [2,3].

From the practical point of view, the corresponding information appears to be necessary for determining correctly the radiation doze during photochemical and photodynamic therapies of a wide range of skin pathologies [4,5]. The series of works [6-9] has become a new stimulus for structural skin changes diagnostics of various diseases. In these studies, the approaches based on the statistical analysis of speckle-images have been suggested. The technique enables identifying reliably relevant qualitative characteristics and obtaining quantitative statistical characteristics of the epidermis structure.

It is known that different biological processes referred to the phenomena of irreversible growth [10] are accompanied with formation of self-similar structures. So, one can suppose that the geometry of rough surfaces of biological origin is generally self-similar and it is formed by a scale-dependent height and angular distributions of micro-irregularities. In other words, in addition to a “classical” statistical approach, a fractal one seems to be also appropriate for the analysis of optical geometric properties of the mentioned objects [11].

At the same time, the problems, which concern early diagnostics of the processes causing structural changes in the skin (e.g., the

developed stages of psoriasis or eczema) and deal with the transformations of angular structure of the upper keratin epidermis layer, have not yet been perfectly studied.

This paper is directed to elaborating polarization reconstruction techniques for the microrelief of rough epidermis surface, as well as further statistical and fractal analyses of its angular structure, which are aimed at early pre-clinic diagnostics of pathological skin changes.

2. Theoretical modelling

2.1. Formation of polarization structure of the object field

Let us consider the skin epidermis as a multilayer flat keratinous epithelium that exhibits optical anisotropy. The electron microscopy data prove that it consists of a large number of tile-like lamellae, or optical microplates, with the average statistical linear sizes of 5–20 μm [12].

Optical properties of local microplate of the epidermis may be characterized using the following Jones matrix [4]:

$$D = \begin{vmatrix} \Delta\rho(\gamma, n) & 0 \\ 0 & 1 \end{vmatrix}. \qquad (1)$$

Here $\Delta\rho(\gamma, n)$ denotes the ratio between the amplitude reflection coefficients $\rho_x(\gamma, n)$ and $\rho_y(\gamma, n)$ that correspond to the orthogonal components E_{ox} and E_{oy} of the illuminating wave amplitude E_o [13], γ is the inclination angle of the epidermis plate and $n \approx 1.46$ the refraction coefficient index of its substance [9].

Analytically, the process of formation of polarization structure at every point r of the object field of such surfaces is described by the matrix equation

$$\begin{pmatrix} E_x(r) \\ E_y(r) \end{pmatrix} = \{D\} \begin{pmatrix} E_{0x} \\ E_{0y} \end{pmatrix}, \qquad (2)$$

where $E_x(r)$ and $E_y(r)$ represent orthogonal components of the complex amplitude $E(r)$ of the reflected radiation.

After solving Eq. (2), one can see that the boundary field of the epidermis surface is polarizationally inhomogeneous. It is formed by an ensemble of linearly polarized zones with the azimuths $\alpha(r)$:

$$\alpha(r) = \frac{1}{2}\arctan\left\{\frac{\sin 2\alpha_0 \Delta\rho(r)\sqrt{1-\Delta\rho(r)^2\cos^2\alpha_0}}{2\Delta\rho(r)^2\cos^2\alpha_0}\right\}, \qquad (3)$$

where α_0 means the polarization azimuth of the illuminating wave.

2.2. Reconstruction of the angular structure of skin surface microrelief

In frame of a single-scattering approximation [13], one can determine the relationship between the azimuth $\alpha(r)$ of homogeneously polarized zone of the object field and the inclination angle γ of the skin epidermis plate. If illumination along the normal of the rough surface is addressed, the equation

$$\gamma(r) = \arcsin\left[u_1 + \left(u_2 + u_3\right)^{1/2} u_4^{-1}\right]^{1/2} \qquad (4)$$

is satisfactory, in which the notations

$$u_1 = n^2 + 1,\ u_2 = \left(n^2+1\right)^2,$$
$$u_3 = \frac{16n^2\tan 2\alpha(r)}{\tan 2\alpha(r) - 1},\ u_4 = \frac{8\tan 2\alpha(r)}{\tan 2\alpha(r) - 1} \qquad (5)$$

are used.

Thus, polarimetry of the object field of skin epidermis provides a possibility for determining/reconstructing the coordinate distribution $\gamma(r)$ of the angular characteristics of its surface microrelief.

2.3. Technique for the analysis of coordinate distributions of optical geometric skin epidermis parameters

Statistical analysis consists in determining histograms of the coordinate distributions $\alpha(r)$ and $\gamma(r)$ and calculating a set of statistical moments of the first (M), second (σ), third (A) and fourth (E) orders:

$$M = \frac{1}{N}\sum_{q=1}^{N}\left|(z)_q\right|, \quad \sigma = \sqrt{\frac{1}{N}\sum_{q=1}^{N}(z)_q^2},$$
$$A = \frac{1}{\sigma^3}\frac{1}{N}\sum_{q=1}^{N}(z)_q^3, \quad E = \frac{1}{\sigma^2}\frac{1}{N}\sum_{q=1}^{N}(z)_q^4, \tag{6}$$

where $(X_{m=1\div800}, Y_{n=1\div600})$ and $N = m \times n$ give a number of pixels of light-sensitive area of CCD camera and $z \equiv \alpha(r)$ or $\gamma(r)$.

In order to classify the coordinate distributions $\alpha(r)$ and $\gamma(r)$, we have used the approach described in [14]. At the first stage, the autocorrelation functions of 2D array (defined by the number $N = m \times n$ of pixels characterizing the receiving area of CCD camera) of the local values $\alpha(r)$ and the corresponding $\gamma(r)$ are being calculated. Then the corresponding power spectra $P(\alpha)$ and $G(\gamma)$ are found and the dependences $\log P(\alpha)$ vs. $\log(r^{-1})$ and $\log G(\vartheta)$ vs. $\log(r^{-1})$ are plotted (with r^{-1} being the spatial frequencies determined by the coordinates r of the object field points and ϑ the incidence angle). Finally, the slopes η_i are calculated for the obtained dependences. The fractal dimension is then defined according to the algorithm

$$D(\alpha) = 3 - \tan\eta_i,$$
$$D(\gamma) = 3 - \tan\eta_i. \tag{7}$$

The coordinate distributions $\alpha(r)$ and $\gamma(r)$ have been classified according to the criteria suggested earlier in the work [15]:

$\alpha(r)$, $\gamma(r)$ are self-similar (fractal), if we deal with a uniquely defined slope η of the log-log dependences of the power spectra $P(\alpha)$ and $G(\vartheta)$ within 2–3 decades of sizes determined by the field point coordinates;

$\alpha(r)$, $\gamma(r)$ are stochastic, if we deal with several different slopes η_i of the log-log dependences of the power spectra $P(\alpha)$ and $G(\vartheta)$ within the mentioned range of the coordinates r_i in the object field;

$\alpha(r)$, $\gamma(r)$ are statistical (random), if we deal with the absence of well-defined slopes of the $\log P(\alpha)$ vs. $\log(r^{-1})$ and $\log G(\vartheta)$ vs. $\log(r^{-1})$ dependences in the whole coordinates range.

3. Experimental studies and discussion

The optical scheme of the experiment is presented in Fig. 1. Linearly polarized radiation of He-Ne laser 1 is transformed into circularly polarized light by a quarter-wave plate 2. Polarizer 3 sets the polarization azimuth α_0 of the illuminating beam. Beam splitter 4 "decouples" optically the illuminating beam and the epidermis object field 5. An objective 6 projects the latter field through analyzer 7 onto the plane of CCD camera 8, which is connected with microprocessor 9.

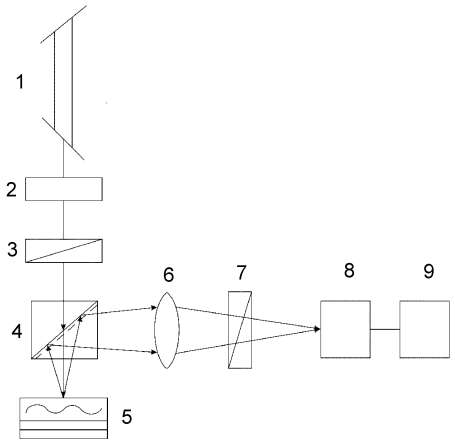

Fig. 1. Scheme of experimental setup.

It should be emphasized that the beam splitter brings distortions into the polarization state of the object field, owing to polarizing impact of the interface. We have taken these changes into account through introducing the matrix that describes laser radiation transmission and reflection by the surfaces of the beam splitter:

$$\mathrm{T} = \begin{vmatrix} \Delta R(\vartheta) & 0 \\ 0 & 1 \end{vmatrix}, \tag{8}$$

where $\Delta R(\vartheta)$ is the ratio of the amplitude reflection and transmission coefficients for the

beam splitter surfaces, which depends on the incidence angle ϑ.

It can be shown that the polarization azimuth α^* of the object field measured at the point with the coordinate r is related to the real value of this object field parameter through the following relation:

$$\alpha(\vartheta) = \\ = \frac{1}{2}\arctan\left[\Delta R(\vartheta)\left(1-\Delta R\left(\vartheta=\pi/4\right)\right)\tan\alpha^*(\vartheta)\right]. \quad (9)$$

Two groups of histological sections of the epidermis layer have been used as investigation objects. Namely, the group "A" (see Fig. 2a) and the group "B" (Fig. 2b) refer respectively to physiologically normal skin and the one that manifests early stages of psoriasis. The thickness of the sections has been 10 μm and so corresponded to the terms of single-scattering approach.

From the medical point of view, such the samples are practically the same (see Fig. 2a and 2b). Applications of common methods of the dark-field microscopy [11], laser profilometers or confocal scanning microscopy [16] do not provide a possibility for differentiating among those surfaces.

Fig. 3 represents the coordinate and statistical distributions of polarization azimuths of the object field for the epidermis of physiologically normal (Fig. 3a) and pathologically changed (Fig. 3b) skin. Basing on the results obtained above, one can see that the boundary fields of the skin epidermis samples of both types are polarizationally inhomogeneous. The azimuth values are randomly distributed (see Fig. 2c and 2d) in the range of 0°–30°. However, the coordinate and statistical polarization structures of the boundary fields peculiar for the samples under study are different.

The polarization chart of pathologically changed skin surface (see Fig. 2b) is more large-scale, when compared with physiologically normal epidermis (Fig. 2a). The average sizes of the zones with similar polarization ($\alpha_i \approx const$) are equal to 15μm and 20μm, respectively.

The distribution of polarization azimuths of the boundary field typical for pathologically changed skin surface is rather equi-probable (Fig. 3d), while the histograms characterizing physiologically normal skin surface are asymmetric (Fig. 3c). The statistical moments of the first (M), second (σ), third (A) and fourth (E) orders describing the 2D distribution of the polarization azimuths are presented in Table 1. Comparative analysis of the statistics of different orders applied to the polarization structure of the boundary field of skin epidermis of both mentioned types testifies that the greatest differences (2–3 times) occur for the asymmetry (A parameter) and the kurtosis (E parameter) that describe $\alpha(r)$ distributions.

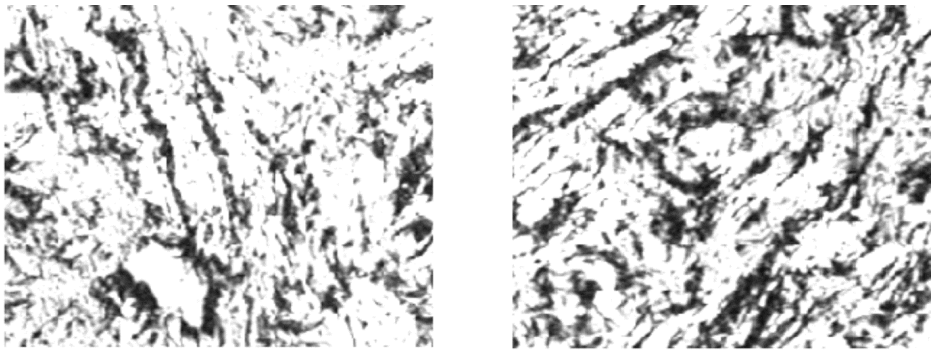

a) **b)**

Fig. 2. Polarization images of physiologically normal (a) and pathologically changed (b) skin epidermis.

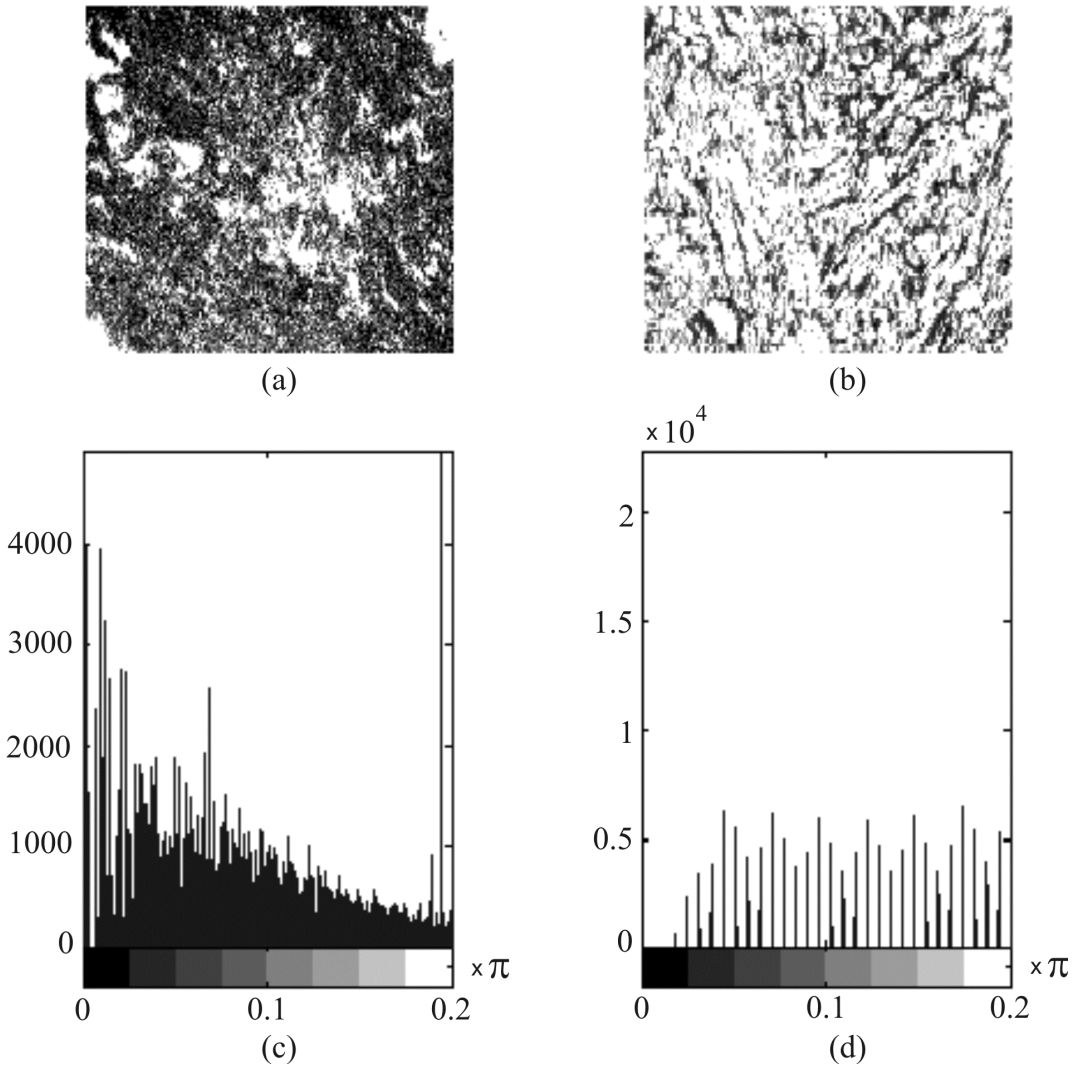

Fig. 3. Coordinate structure (a, b) and the corresponding histograms (c, d) of polarization azimuths of the boundary field typical for the epidermis surfaces of physiologically normal (a, c) and pathologically changed (c) skin.

The peculiarities of the two coordinate distributions $\alpha(r)$ are illustrated by the dependences $\log P(\alpha)$ vs. $\log P(r^{-1})$ depicted in Fig. 4a and 4b, respectively. One can see that the boundary fields of physiologically normal skin epidermis samples are characterized by practically self-similar (fractal) structure. The slopes η_i of the log-log dependences of the power spectra $P(\alpha)$ are invariable with the accuracy of 3–5% within at least 2–3 decades of the object field point coordinates (2–1000 μm). We have performed linear approximation of

Table 1. Statistics of the first to fourth orders for the polarization azimuths.

Statistics of epidermis (field)	Physiologically normal (36 samples)	Pathologically changed (34 samples)
M_α, %	0.806±6	0.734±4
σ_α, %	0.349±4	0.498±5
A_α, %	16.75±10	5.689±12
E_α, %	95.8±15	37.8±11

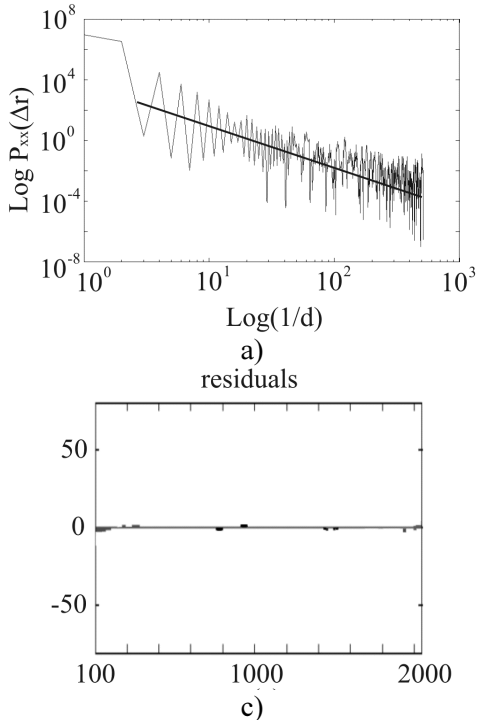

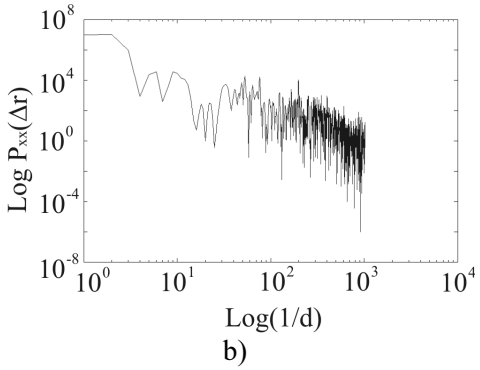

Fig. 4. Log-log plots for the power spectra of polarization azimuths of the boundary field in case of physiologically normal (a) and pathologically changed (b) skin. The residuals are shown in part (c).

log$P(\alpha)$ vs. log$P(r^{-1})$ dependences, using the standard least-square routine, and then determined the slopes η_i. For better clarity, the corresponding lines are depicted like the slopes of log$P(\alpha)$ vs. log$P(r^{-1})$ dependences.

The processes of pathological changes of the skin surface structure manifest themselves in "destroying" both the fractal structure and "statisticity" of the coordinate distributions $\alpha(r)$. Then a single slope η_i of the dependences log$P(\alpha)$ vs. log$P(r^{-1})$ cannot be practically found.

The possibilities for polarization reconstruction of the surface microrelief for the

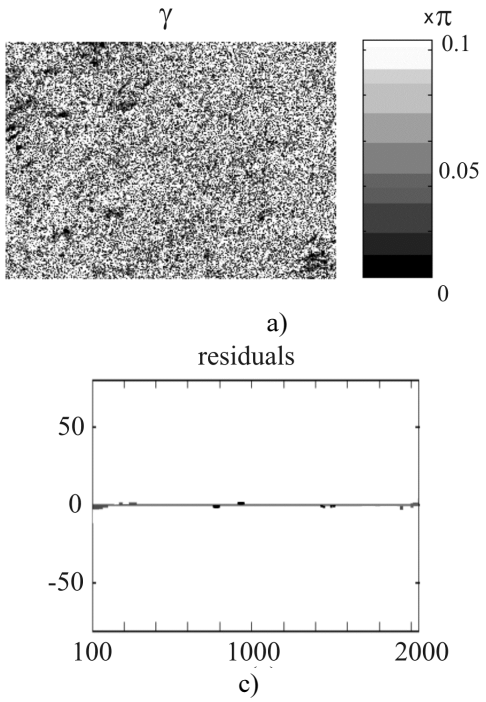

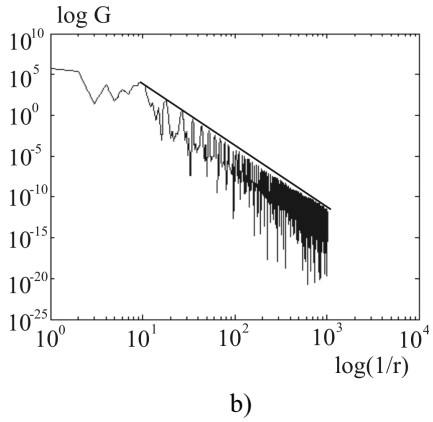

Fig. 5. Coordinate distribution of the inclination angles of epidermis plates for physiologically normal skin (a) and log-log plots of their power spectra (b). The residuals are shown in part (c).

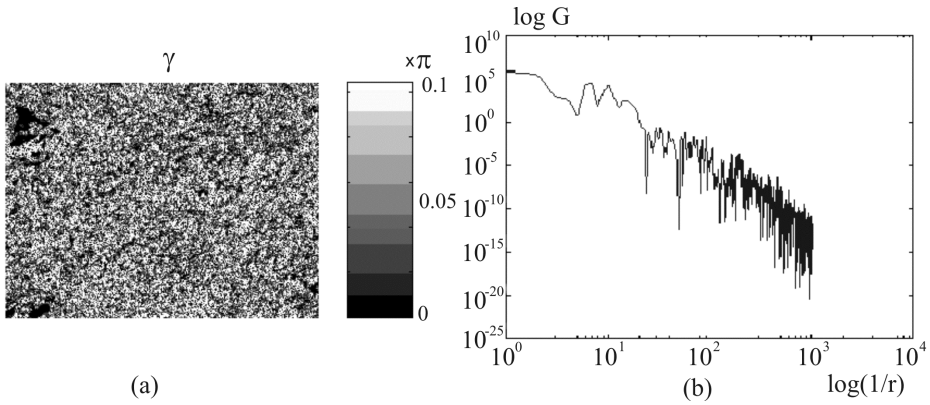

Fig. 6. Coordinate distribution of the inclination angles of epidermis plates for pathologically changed skin (a) and log-log plots of their power spectra (b).

cases of physiologically normal and pathologically changed skin epidermis are illustrated in Fig. 5 and 6, respectively. It is easy to see that the inclination angles $\gamma(r)$ of micro-irregularities typical for the both types of skin epidermis surfaces change in the range of 0°–20° (see Fig. 5a and 6a). This correlates well with the results of direct microscopic investigations of the inclination angles performed for microplates of skin epidermis layer, using the light section technique [10].

Rough surface of the healthy skin epidermis is shaped of plates with the average size of 7μm (see Fig. 5a). Pathologically changed skin epidermis plates are practically 3 times larger (Fig. 6a). The information obtained for the statistical moments that describe the $\gamma(r)$ distributions for different tissues proves (see Table 2) that the differences between the fourth-order statistical moments for the physiologically normal and pathologically changed epidermis surfaces reach one order of magnitude for the values $E(\gamma)$. Besides, the microrelief of the rough surface of the healthy skin epidermis has a clear self-similar (fractal) structure (see Fig. 5b). At the same time, a random distribution of the inclination angles of the epidermis surface microelements is typical for the pathologically changed skin (see Fig. 6b).

4. Summary

Let us finally summarize the main results obtained in the present work:

1. The polarization technique for reconstructing the angular structure of the skin surface is elaborated and experimentally tested. It is based on optical modelling of that surface by a set of quasi-flat epidermis plates.

2. It is shown that the kurtosis of the coordinate distributions for the inclination angle of epidermis plates, whose value changes within one order of magnitude, is the most sensitive to the angular structure changes occurring in the skin surface microrelief.

3. Optical geometric properties of the epidermis surface typical for physiologically

Table 2. Statistics of the first to fourth orders for the inclination angles.

Statistics of epidermis (surface)	Physiologically normal (36 samples)	Pathologically changed (34 samples)
M_γ, %	0.806±3	0.734±3
σ_γ, %	0.349±4	0.498±5
A_γ, %	16.75±11	2.689±10
E_γ, %	35.8±20	3.8±17

normal skin reveal a self-similar (fractal) structure.

4. The processes of pathological changes in the biological tissue result in the surfaces, for which a random angular structure of the microrelief is typical.

References

1. A.G.Ushenko and V.P.Pishak in 'Coherent-Domain Optical Methods. Biomedical Diagnostics, Environmental and Material Science' (Ed. V.Tuchin), Kluwer Academic Publishers, 2004. – 67–93.
2. J.M.Schmitt, G.X.Zhou, E.C.Walker and R.T.Wall J. Opt. Soc. Am. A **7** 2141–2153 (1990).
3. R.Graaff, A.C.M.Dassel, M.H.Koelink, F.F.M. de Mul, J.G.Aarnoudse and W.G.Zijlstra Appl. Opt**. 32** 435–447 (1993).
4. M.J.C. van Gemert, D.J.Smithies, W.Verkruysse, T.E.Milner and J.S.Nelson Phys. Med. Biol. **42** 41–50 (1997).
5. Laser-induced intestinal thermotherapy (Ed. G.Muller and A.Roggan), Bellingham, SPIE (1995).
6. Pishak V.P., Gryhoryshyn P. and Yermolenko S. Proc. SPIE **3317** 418–425 (1997).
7. A.G.Ushenko Laser Physics **10** 1–7 (2000).
8. A.G.Ushenko Laser Physics **10** 1143–1149 (2000).
9. Yu.A.Ushenko Proc. SPIE **5477** 506–512 (2004)
10. Feder J. Fractals (New York: Plenum Press) 1988.
11. E.Marx and T.V.Vorburger Appl. Opt. **29** 3613–3626 (1990).
12. A.Gerrard and J.M.Burch Introduction to matrix methods in optics (New York: John Wiley & Sons) 1975.
13. Ushenko A.G. Opt. Eng. **34** 1088–1093 (1995).
14. Y.P.Zhao, C.F.Cheng, G.C.Wang and T.M.Lu Surface Sci. Lett. **409** L703–L708 (1998).
15. D.J.Whitehouse Wear **249** 345–353 (2001).
16. Somekh M.G., Valera M.S. and Appel R.K. Proc. SPIE. **1647** 28–38 (1992).